Constraining the solar neutrino survival probability curve by using ^{6}Li, ^{7}Li, ^{12}C, ^{18}O, ^{19}F, and ^{42}Ca nuclear targets

Y. Fujita,[1,2,*] K. Zuber,[3,†] and H. Fujita[1]

[1]Research Center for Nuclear Physics, Osaka University, Ibaraki, Osaka 567-0047, Japan
[2]Department of Physics, Osaka University, Toyonaka, Osaka 560-0043, Japan
[3]Institute for Nuclear and Particle Physics, Technische Universität Dresden, D-01069 Dresden, Germany

(Received 8 October 2020; accepted 24 June 2021; published 23 July 2021)

Precise measurement of the survival probability P_{ee} of solar electron neutrino (ν_e) as a function of its energy $[P_{ee}(E_{\nu e})]$ is one of the key issues in neutrino physics. Current P_{ee} data, due to their limited accuracy, still allow for nonstandard interactions (NSIs) to be alternatives to the standard one, which is based on the MSW-LMA prediction. In order to determine P_{ee} values at several values of $E_{\nu e}$ with higher accuracy, we propose to use several target nuclei with different threshold energies for ν_e detection. We examined charged-current (CC) responses of various nuclei seeking the ones: (a) having large and concentrated Gamow-Teller (GT) transition strength in the low excitation-energy region, and (b) having appropriate and a variety of reaction Q values, i.e., ≈1 to 17 MeV, in the (ν_e, e^-) reaction. As a result, we found that systematic solar ν_e measurements with target nuclei ^{6}Li, ^{7}Li, ^{12}C, ^{18}O, ^{19}F, and ^{42}Ca can put strong constraints on the $P_{ee}(E_{\nu e})$ curve and thus on these NSI models. In addition, we notice that three of these nuclei, ^{6}Li, ^{7}Li, and ^{12}C, have large and concentrated neutral-current (NC) responses with detection threshold-energies of 3.56, 0.48, and 15.11 MeV, respectively. Note that the NC measurement is flavor independent. Thus, the measured results should represent the original strength of ν_e from the Sun.

DOI: 10.1103/PhysRevD.104.013004

I. INTRODUCTION

Since the experimental finding of the continuous β decay spectra observed about a century ago and its solution by Pauli in 1930 [1] proposing a new lepton nowadays called neutrino that shares energy with the emitted electron, the physics on neutrino has expanded enormously. Shortly after, energy production via fusion reactions in stars has been proposed by von Weizsäcker and Bethe [2–5]. Pontecorvo followed the neutrino hypothesis of Pauli and suggested that neutrino (i.e., the electron neutrino ν_e) can also be produced in the Sun. In addition, for the detection of ν_e, he even proposed to use the reaction of ν_e on the target nucleus ^{37}Cl into ^{37}Ar [6]. Many years later, this led into the Homestake chlorine experiment which successfully measured solar ν_e for the first time [7,8]. Important finding of this experiment is that they observed a reduced number of ν_es than expected from the standard solar modeling.

Improved radiochemical experiments have been performed based on the ν_e reaction on the target nucleus ^{71}Ga into ^{71}Ge. Owing to the small reaction Q value of 0.23 MeV, even the low-energy pp-ν_e, which is dominant, could be detected. Measurements were performed by the GALLEX [9,10], GNO [11], and SAGE [12] experiments and again they all confirmed a deficit of the ν_e flux. In addition, the Kamiokande experiment and its upgrades, measuring higher energy ^{8}B-ν_e, also confirmed the deficit [13].

In the SNO experiment, target nucleus deuteron has been used, which allowed a simultaneous neutral-current (NC) and charged-current (CC) measurement [14]. In the CC measurement, they also found the deficit of the ν_e flux. On the other hand, in the NC measurement, which is flavour blind and all kinds of neutrinos contribute, the total number of detected neutrinos was in agreement with the total number of solar ν_es expected from the standard solar modeling. This finding was a strong evidence that a neutrino can change its flavor.

Further measurements have been made by Borexino. This solar neutrino detector is based on an ultrapure liquid scintillator. They could observe almost all kinds of ν_es produced in the pp-chain (except the ν_e from the hep reaction) by using ν_e–e^- elastic scattering [15]. On the basis of their observation, values of ν_e survival probability P_{ee}, i.e., the probability of ν_es produced in the Sun still being detected as ν_es on the Earth, were derived at four values of ν_e energy ($E_{\nu e}$) [15–17] (see Fig. 1). Although the uncertainties are rather large, we see that the values of P_{ee} are more or less constant in the low $E_{\nu e}$ region and they become smaller at higher $E_{\nu e}$ region. The constant but

*fujita@rcnp.osaka-u.ac.jp
†kai.zuber@tu-dresden.de

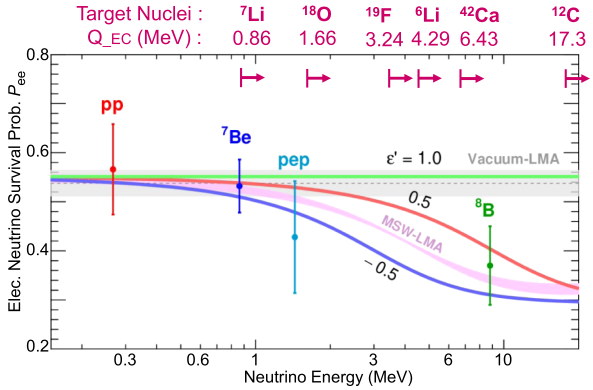

FIG. 1. Theoretical predictions and experimental data for the ν_e survival probability P_{ee} as a function of its energy $E_{\nu e}$ (original figure: from [20]). Theoretical prediction from the MSW-LMA solution is shown by the pink band, where uncertainties of oscillation parameters are included. Also shown are the MSW-LMA + nonstandard interaction (NSI) solutions for $\epsilon' = -0.5, +0.5$, and $+1.0$. Four experimental P_{ee} values from the latest Borexino analysis under the HZ-SSM assumption are plotted for pp-ν_e, ^{7}Be-ν_e, pep-ν_e, and also ^{8}B-ν_e [15]. In addition to these, a P_{ee} value for ^{7}Be-ν_e is available from KamLAND-Zen measurement [21], and values for ^{8}B-ν_e are available from Super-Kamiokande [13] and SNO [22]. For the six candidates of target nuclei to be discussed in this paper, the threshold energies for ν_e detection, i.e., the $Q_{\rm EC}$ values, are indicated.

reduced values of $P_{ee} \approx 0.55$ in the $E_{\nu e} < 1$ MeV region can be qualitatively explained by the effects of vacuum oscillation. On the other hand, the smaller P_{ee} values at higher energies (>1 MeV) shows that the Mikheyev-Smirnov-Wolfenstein (MSW) effect, i.e., the matter effect inside the Sun [18,19], should also be taken into account.

The measured data points can constrain the shape of the theoretical $P_{ee}(E_{\nu e})$ curve; we see in Fig. 1 that they are, to some extent, consistent with the $P_{ee}(E_{\nu e})$ curve derived by the MSW-LMA (large mixing angle) solution [20]. However, given the large experimental uncertainty, there still remains some room for beyond Standard Model (BSM) physics, like the one assuming nonstandard interaction (NSI) (see, e.g., Ref. [23] and references in [20]).

Seeking a better accuracy in the $P_{ee}(E_{\nu e})$ measurement, here we propose to use several target nuclei with different ν_e-detection threshold energies. In addition, we request each target nucleus to have compact and strong ν_e-detection response in the low excitation-energy (E_x) region. As will be discussed in detail in Sec. IV, we find, in total, six candidates of target nuclei having these properties by investigating the whole nuclear chart. Their Q values cover the full ν_e energy range of our interest, i.e., from 0.9 MeV up to 17 MeV.

Note that the very light particle ν_e can induce mainly the angular-momentum-transfer $\Delta L = 0$ components of the CC-induced transition. In nuclear physics, the corresponding transitions are well defined; they are the Gamow-Teller (GT) and Fermi transitions. Therefore, we discuss the ν_e response-function of each target nucleus quantitatively in terms of the distributions of B(GT) and B(F) strengths, i.e., the reduced GT and Fermi transition strengths.

II. NUCLEAR PHYSICS BACKGROUND

A. Solar neutrino induced reaction and β-decay

Solar electron neutrinos (solar ν_es) can be detected by using CC-induced reactions, i.e., the charge-exchange reactions (CE reactions) on target nuclei $^A[\mathrm{Z}]_N$. The reaction is expressed by

$$^A[\mathrm{Z}]_N(\nu_e, e^-)^A[\mathrm{Z}+1]_{N-1}, \quad (1)$$

where A is the mass number, Z the proton number, N the neutron number, and $A = Z + N$. [Z] and [$Z + 1$] are the elements with proton numbers Z and $Z + 1$, respectively. The active interaction here is the weak interaction. The Q value in the ν_e-induced CE reaction is the β^+-decay $Q_{\rm EC}$ value of the final nucleus $^A[\mathrm{Z}+1]_{N-1}$. Therefore, only those ν_es having energies $E_{\nu e} > Q_{\rm EC}$ are detected by a target nucleus.

In the reaction shown by Eq. (1), ν_es make mostly Fermi and GT transitions with target nuclei. These transitions are caused by the simple isospin (τ) and spin-isospin ($\sigma\tau$) operators, respectively [24,25]. They are called the "allowed transitions" in β decays due to their $\Delta L = 0$ nature.

The τ-operator can change a neutron in a nucleus into a proton and vice versa. Thus, its contribution is essential in β decays and also in the ν_e-induced CE reactions. It is noted that τ-operator cannot change the spacial nor spin structures in nuclei. As a result, the total reduced Fermi transition strength, i.e., $B(\mathrm{F}) = N - Z$, concentrates, in principle, in the transition to the isobaric analog state (IAS). Note that the value of B(F) shows the sensitivity for detecting ν_e by means of Fermi transition.

In GT transitions caused by the $\sigma\tau$-operator, change in spin structure is additionally allowed. Therefore, the available total sum of the GT strengths, given by the Ikeda GT sum-rule (GT-SR) [26]

$$\Sigma B(\mathrm{GT}^-) - \Sigma B(\mathrm{GT}^+) = 3(N - Z), \quad (2)$$

can be distributed into a number of GT-excited states (GT states) in the final nuclei, where $B(\mathrm{GT}^\pm)$ are the reduced GT transition strengths in the $\beta^\pm$ directions, respectively. Note that the value of B(GT) shows the sensitivity for detecting ν_e by means of GT transition.

B. Gamow-Teller responses in nuclei

Since the 1980s, it was gradually recognized that GT and also Fermi transitions can be studied by means of hadronic CE reactions [25]. Note that β decays can study GT transitions only inside the β-decay Q windows, but they can give absolute values of $B(\mathrm{GT})$. On the other hand, hadronic CE reactions can study GT transitions to higher E_x region, but only relative values of $B(\mathrm{GT})$ can be studied. Thus, β decay and hadronic CE reaction are complementary [25].

It was found that hadronic CE reactions, such as (p, n) or $(^3\mathrm{He}, t)$ reactions (here t stands for triton, i.e., $^3\mathrm{H}$), performed at intermediate incoming energies of $E_i >$ 100 MeV/nucleon selectively excite GT transitions with $\Delta L = 0$ at the scattering angle $\Theta \approx 0°$ [25,27]. Note that under these conditions, the reaction mechanism is simple. As a result, although there are some exceptions, a close proportionality between the cross sections at $\Theta = 0°$ and the $B(\mathrm{GT})$ values

$$\sigma(0°) \simeq \hat{\sigma}^{\mathrm{GT}}(0°)B(\mathrm{GT}), \tag{3}$$

has been empirically established [25,27–32]. Here, $\hat{\sigma}^{\mathrm{GT}}(0°)$ is the unit GT cross section at $\Theta = 0°$. Note that $\Delta L = 0$ transitions are most prominent at $\Theta = 0°$.

Here, the $(^3\mathrm{He}, t)$ reaction on a target nucleus $^A[\mathrm{Z}]_N$ can be written as

$$^A[\mathrm{Z}]_N(^3\mathrm{He}, t)^A[\mathrm{Z}+1]_{N-1}, \tag{4}$$

and we see a similarity with Eq. (1), although this reaction is caused by the hadronic strong interaction.

As discussed, GT transition strength can be distributed in a number of states. In addition, the distributions are largely dependent on the structures of individual nuclei and some of them are extreme [25,28,33]. In order to deduce the nuclear response caused by the (ν_e, e^-) CE reaction, let us discuss the GT response in the β^--direction that can be studied by the (p, n)-type $(^3\mathrm{He}, t)$ reaction. Note that in this reaction, approximately one-order-of-magnitude better energy resolution can be achieved compared to the traditionally used (p, n) reaction [25]. As a result, even weak GT transitions are well studied.

One of the extreme structures of GT excitations, but well studied in (p, n)-type CE reactions since the 1980s, is the GT resonance (GTR) [28,34]. GTR structures are commonly observed in higher E_x regions ($E_x \approx$ 5–15 MeV) of neutron-excess ($N > Z$) nuclei. They carry a large part of the GT strength allowed by the GT-SR value [see Eq. (2)] and show resonancelike structures. In the $^{37}_{17}\mathrm{Cl}_{20}(^3\mathrm{He}, t)^{37}_{18}\mathrm{Ar}_{19}$ reaction, a GTR with a bumplike structure has been observed as fragmented states in the $E_x \approx 8$ MeV region of $^{37}\mathrm{Ar}$ [35] [see Fig. 2(a)]. As a result, only a small portion of GT strength remains for the states in the $E_x < 5$ MeV region.

On the other hand, there are several extreme cases in which most of the observed GT strength is concentrated in one or two low-E_x states. Typical examples are the low-energy super GT (LeSGT) states [33,36–38]. The LeSGT state is the lowest GT state in the final nucleus and carries a large part of the GT-SR strength. In the $^{18}_{8}\mathrm{O}_{10}(^3\mathrm{He}, t)^{18}_{9}\mathrm{F}_9$ CE reaction, a LeSGT state has been observed as a pronounced and sharp ground state (g.s.) in $^{18}\mathrm{F}$ [36]. It carries a very large $B(\mathrm{GT})$ value of 3.08 [see Fig. 2(b)]. Note that this value is two orders-of-magnitude larger than the $B(\mathrm{GT})$ value of 0.03 in the $^{37}\mathrm{Cl}$ g.s. $\to$ $^{37}\mathrm{Ar}$ g.s. GT transition [35].

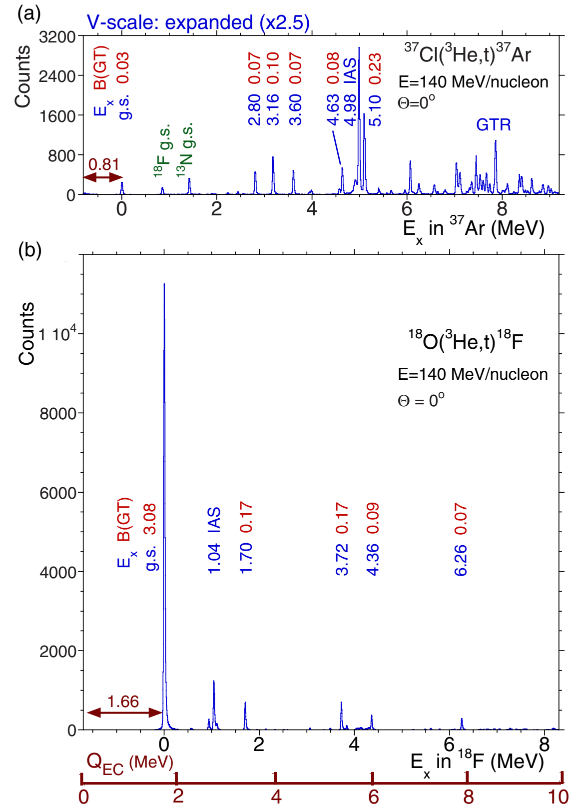

FIG. 2. Spectra of (a) $^{37}\mathrm{Cl}(^3\mathrm{He}, t)^{37}\mathrm{Ar}$ [35] and (b) $^{18}\mathrm{O}(^3\mathrm{He}, t)^{18}\mathrm{F}$ [36] CE reactions measured at $\Theta = 0°$ with an energy resolution of $\approx$30 keV. The origins of the E_x axes are shifted by the amount of g.s.–g.s. Q_{EC} values, i.e., 0.81 and 1.66 MeV for the $^{37}\mathrm{Ar}$ and $^{18}\mathrm{F}$ nuclei, respectively. As a result, the minimum energy of ν_e needed to excite each state, i.e., the Q_{EC} value, can be seen directly. The $B(\mathrm{GT})$ value derived by using Eq. (3) is given for each GT state. In the $^{37}\mathrm{Ar}$ spectrum [(a)], the vertical scale is expanded [in terms of $B(\mathrm{GT})$] by a factor of 2.5 compared to that of (b). In the $^{18}\mathrm{O} \to {}^{18}\mathrm{F}$ transition [(b)], the GT strength is much concentrated in the $J^\pi = 1^+_1$ g.s., i.e., the LeSGT state [36]. The IAS at 1.04 MeV is excited with $B(\mathrm{F}) = N - Z = 2$.

III. FOR THE ACCURATE STUDY OF $P_{ee}(E_{\nu e})$

Seeking a better accuracy in the study of $P_{ee}(E_{\nu e})$, we start with a short review of the representative ν_e-detection projects from a viewpoint of GT responses of target nuclei used in them.

In the Homestake experiment [7], ν_es were detected by the $^{37}_{17}\mathrm{Cl}_{20}(\nu_e, e^-)^{37}_{18}\mathrm{Ar}_{19}$ CE reaction taking the advantage of small Q_{EC} value of 0.81 MeV. As we have seen, the CC response of ^{37}Cl for ν_e can be examined by the ^{37}Cl(^{3}He, t)^{37}Ar reaction at $\Theta = 0°$ [Fig. 2(a)]. With the exception of the 4.98 MeV state, which is known to be the IAS of ^{37}Cl g.s. carrying the total Fermi transition strength of $B(\mathrm{F}) = N - Z = 3$ and a weak GT transition strength of $B(\mathrm{GT}) = 0.06$ [35], other states carrying the GT strength are fragmented and weak in ^{37}Ar [35]. In particular, all GT states up to $E_x = 5$ MeV have small $B(\mathrm{GT})$ values of ≤ 0.1. For example, the g.s. carries a very small $B(\mathrm{GT})$ of 0.03. Therefore, we see that the detection efficiency of ^{37}Cl-based ν_e detectors should be low for low-energy ν_es. In addition, the GT response of ^{37}Cl for ν_e in total is very complicated as a function of $E_{\nu e}$. Therefore, with the data from a ^{37}Cl-based ν_e detector, it seems it is almost impossible to decompose the obtained energy spectra into the number of ν_e as a function of $E_{\nu e}$.

In the projects GALLEX [9,10], GNO [11], and SAGE [12], one of the middle heavy nuclei ^{71}Ga was used as the target nucleus of their ν_e detectors. Owing to the very small reaction Q_{EC} value of 0.23 MeV of the $^{71}_{31}\mathrm{Ga}_{40}(\nu_e, e^-)^{71}_{32}\mathrm{Ge}_{39}$ CE reaction, even the main part of the pp-ν_e was detected. However, as we can see from the ^{71}Ga(^{3}He, t)^{71}Ge spectrum given in Ref. [39], the GT strength distribution in ^{71}Ge is even more fragmented than in ^{37}Ar. In addition, the GT strength is moved up more in the GTR region. Therefore, we also see that ^{71}Ga-based ν_e detectors are not appropriate for the purpose of deriving the $P_{ee}(E_{\nu e})$ curve.

In the Borexino measurement, ν_e–e^- elastic scattering is used. Therefore, the response of their detector as a function of $E_{\nu e}$ is more or less linear. As discussed, using this simple response, they could derive the P_{ee} values for ν_es emitted in the pp-, ^{7}Be-, pep-, and ^{8}B-processes [20]. However, it seems that the derivation of P_{ee} values is still not easy; the contributions of all of the ν_e-producing processes having their own ν_e intensity distributions (see Fig. 3) should be taken into account in a single overall analysis. As we see in Fig. 1, the P_{ee} values derived at four $E_{\nu e}$ values are associated with relatively large uncertainties.

On the basis of the discussions given above, we now propose to use several target nuclei having following properties for the $P_{ee}(E_{\nu e})$ study:

(a) target nuclei should have compact response functions; strengths of GT (and also Fermi) transitions should be concentrated in a single or at most a few excited states in the low-E_x region,

(b) they should have appropriate Q_{EC} values in the range of ≈ 1–17 MeV to study P_{ee} at different $E_{\nu e}$.

IV. NUCLEI HAVING CONCENTRATED GT AND FERMI TRANSITION STRENGTHS

We discuss here the properties of GT and also Fermi transitions for the six candidates of target nuclei. They are, in the order of increasing Q_{EC} value, $^7_3\mathrm{Li}_4$, $^{18}_8\mathrm{O}_{10}$, $^{19}_9\mathrm{F}_{10}$, $^6_3\mathrm{Li}_3$, $^{42}_{20}\mathrm{Ca}_{22}$, and $^{12}_6\mathrm{C}_6$. Note that each of them can detect the ν_es with energies higher than its Q_{EC} value. These nuclei, in total, cover the Q_{EC} range from 0.9 up to 17 MeV. From Fig. 3, we can identify which fusion processes in the Sun can be studied by each target nucleus.

For the discussions given below, the nuclear structure data compiled in Refs. [40,41] are used.

A. GT and Fermi response of $^7_3\mathrm{Li}_4$

The g.s.–g.s. transition of $^7_3\mathrm{Li}_4(\nu_e, e^-)^7_4\mathrm{Be}_3$ CE reaction has a small Q_{EC} value of 0.86 MeV, as we see in Fig. 4. Nuclei ^{7}Li and ^{7}Be are the $T_z = \pm 1/2$ mirror nuclei, where T_z is the z component of isospin T and defined by $T_z = (N - Z)/2$ (in the definition of nuclear physics). In mirror nuclei, proton number Z and neutron number N are reversed. Therefore, as for the strong interaction is concerned, they are the same nuclei, and thus, their nuclear structures should be identical. The action of the electromagnetic (EM) interaction (Coulomb force), however, is

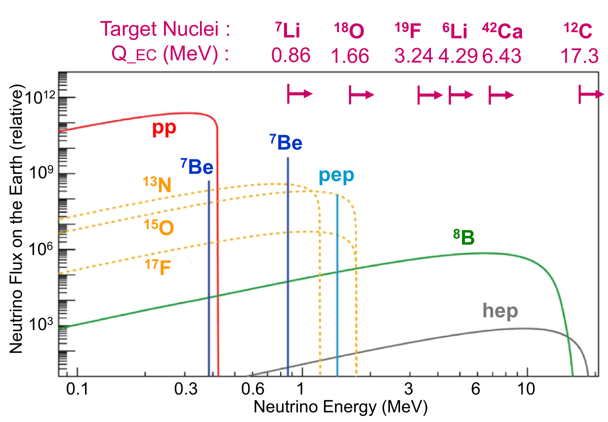

FIG. 3. The flux of solar ν_es from various fusion processes as a function of $E_{\nu e}$. The Q_{EC} values of candidates for target nuclei are indicated.

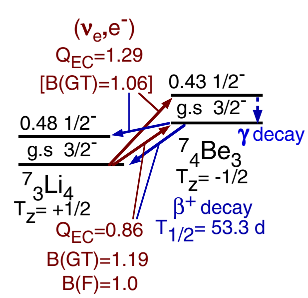

FIG. 4. Energy-level diagram and GT and Fermi transitions in $A = 7$ nuclei. Properties of excitations caused by the ^{7}Li(ν_e, e^-)^{7}Be CE reaction are indicated in red. Decay properties of the states in ^{7}Be are shown in blue. The strength [$B(\mathrm{GT}) = 1.06$] in the square brackets given for the GT transition from the ^{7}Li g.s. to the ^{7}Be 0.43 MeV state is borrowed from that of the mirror (isospin analogous) GT transition studied in the β^+ decay of the ^{7}Be g.s. to the ^{7}Li 0.48 MeV state.

different and thus symmetry of their structures can be broken to some extent.

The experimentally obtained $^7\mathrm{Li}(p,n)^7\mathrm{Be}$ spectrum measured at the scattering angle $\Theta = 0°$ and at an intermediate incoming energy of $E_p = 160$ MeV [42] shows that only two states are excited, i.e., the g.s. and the 0.43 MeV state of ^{7}Be. Angular distribution analysis showed that both of them are excited by $\Delta L = 0$ transitions, indicating that these states are excited by Fermi and/or GT transitions.

Since ^{7}Li and ^{7}Be are mirror nuclei, the Fermi transition strength of $B(\mathrm{F}) = N - Z = 1$ should be concentrated in the g.s.–g.s. transition. The contribution of the GT transition in this g.s.–g.s. transition can be derived by analyzing the β^+-decay data of ^{7}Be into ^{7}Li. The obtained $B(\mathrm{GT}) = 1.19$ is large.

In the $^7\mathrm{Li}(\nu_e, e^-)^7\mathrm{Be}$ CE reaction, the 0.43 MeV state is purely excited by the GT transition. A large $B(\mathrm{GT})$ value of 1.06 is estimated assuming the isospin symmetry of analogous GT transitions between the $T_z = \pm 1/2$ mirror nuclei (see the caption of Fig. 4). By detecting the 0.43 MeV γ ray, the GT excitation of the 0.43 MeV, $J^\pi = 1/2^-$ state in ^{7}Be with a $Q_{\mathrm{EC}} = 1.29$ MeV is identified. The β^+ decay of the ^{7}Be g.s. can be studied by detecting the 0.51 MeV annihilation γ.

The target nucleus ^{7}Li is attractive, because it is also sensitive to NC excitation. In the $T_z = \pm 1/2$ mirror nuclei ^{7}Li and ^{7}Be, the 0.48 MeV state in ^{7}Li is the analogous state of the 0.43 MeV state in ^{7}Be, where we know that the latter is excited with a large $B(\mathrm{GT})$ value of 1.06 from the g.s. of ^{7}Li. Therefore, the 0.48 MeV state in ^{7}Li should also be strongly excited by neutrinos with all flavors by means of the spin-$M1$ excitation (inelastic scattering) caused, like the GT transition, by the $\sigma\tau$ operator [25]. The excitation of the ^{7}Li, 0.48 MeV state is identified by the study of the 0.48 MeV γ ray.

B. GT and Fermi response of $^{18}_{8}\mathrm{O}_{10}$

The Fermi and GT transitions are separated when they start from nuclei with even Z and even N numbers (e-e nuclei). As we have seen in Fig. 2(b), the main part of the GT strength is concentrated in the $^{18}_{8}\mathrm{O}_{10}, 0^+$ g.s. $\rightarrow$ $^{18}_{9}\mathrm{F}_9, 1^+$ g.s. transition. As discussed, this strong transition is the LeSGT transition. In Fig. 5, we see that the associated $B(\mathrm{GT})$ value is very large [$B(\mathrm{GT}) = 3.08$], where the $Q_{\mathrm{EC}} = 1.66$ MeV. This $B(\mathrm{GT})$ value is obtained from that of the β^+ decay of the ^{18}F, 1^+ g.s. to the ^{18}O, 0^+ g.s. after correcting the difference of spin Clebsch-Gordan (CG) coefficients associated with the transitions for reversed directions. The 1.04 MeV, 0^+ IAS in ^{18}F is excited by the Fermi transition with the strength of $B(\mathrm{F}) = 2$.

By detecting the 1.04 MeV γ ray, the excitation of the IAS with a $Q_{\mathrm{EC}} = 2.70$ MeV is identified. The β^+ decay of

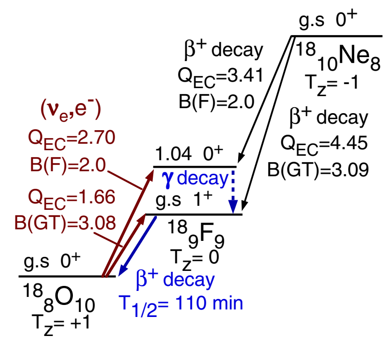

FIG. 5. Energy-level diagram and the prominent GT and Fermi transitions in $A = 18$ nuclei. Properties of $T_z = +1 \rightarrow 0$ transitions caused by the $^{18}\mathrm{O}(\nu_e, e^-)^{18}\mathrm{F}$ CE reaction are indicated in red. Decay properties of ^{18}F are shown in blue. Properties of $T_z = -1 \rightarrow 0$ transitions from ^{18}Ne to ^{18}F are shown in black. We see that the $T_z = \pm 1 \rightarrow 0$ mirror g.s.–g.s. GT transitions have $B(\mathrm{GT})$ values of 3.08(2) and 3.09(3), respectively; they are consistent within uncertainties.

the ^{18}F g.s. can be studied via the detection of the 0.51 MeV annihilation γ.

One of the attractive features of the target nucleus ^{18}O, with the Q_{EC} value of 1.66 MeV, in combination with the target nucleus ^{7}Li, with the Q_{EC} value of 0.86 MeV, is the possibility of studying three kinds of CNO-ν_es in detail. They are the ^{13}N-ν_e, ^{15}O-ν_e, and ^{17}F-ν_e having maximum $E_{\nu e}$ values of 1.12, 1.73, and 1.74 MeV, respectively (see Fig. 3). The ^{7}Li-based detector is sensitive to all of them. On the other hand, the ^{18}O-based detector can detect only the ^{15}O-ν_e and ^{17}F-ν_e.

C. GT and Fermi response of $^{19}_{9}\mathrm{F}_{10}$

The target nucleus $^{19}_{9}\mathrm{F}_{10}$ and the final nucleus $^{19}_{10}\mathrm{Ne}_9$ are $T_z = \pm 1/2$ mirror nuclei. Therefore, just like the case of $A = 7$ mirror nuclei, both Fermi and GT transitions can contribute in the g.s.—g.s. transition, where the Fermi transition strength $B(\mathrm{F}) = N - Z = 1$ (see Fig. 6).

We see that the GT + Fermi response of ^{19}F is very simple. The $^{19}\mathrm{F}(p,n)^{19}\mathrm{Ne}$ spectrum measured at $\Theta = 0°$ and at an intermediate incoming energy of $E_p = 120$ MeV

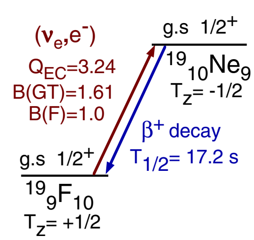

FIG. 6. Energy-level diagram and the prominent GT + Fermi g.s.–g.s. transitions in $A = 19$ nuclei. Properties of the transition caused by the $^{19}\mathrm{F}(\nu_e, e^-)^{19}\mathrm{Ne}$ CE reaction are indicated in red. Decay properties of the g.s. of ^{19}Ne are shown in blue.

(energy resolution $\Delta E \approx 400$ keV) [43] shows that only one state, i.e., g.s. of ^{19}Ne, dominates the spectrum. In addition, recent high-resolution ^{19}F(^{3}He, t)^{19}Ne measurement ($\Delta E \approx 40$ keV) confirmed that the higher E_x GT states are all very weak [44].

The contribution of GT strength in this strong g.s.–g.s. transition can be studied by analyzing the β^+-decay data of ^{19}Ne into ^{19}F. As a result, we notice that a large B(GT) value of 1.61 coexists with the Fermi transition strength of $B(\mathrm{F}) = 1$, as we see in Fig. 6.

The Q_{EC} value is 3.24 MeV. Therefore, the ^{8}B-ν_e and hep-ν_e above this energy can be detected (see Fig. 3). The β^+ decay of the ^{19}Ne g.s. can be studied by the detection of 0.51 MeV annihilation γ.

D. GT response of $^6_3$Li$_3$

As shown in Fig. 7, the $Z = N = 3$ odd-odd nucleus ^{6}Li has $T_z = 0$, and thus the 1^+ g.s. has $T = 0$. Since no analogous state of the ^{6}Li g.s. with $T = 0$ is expected in the $T_z = -1$ nucleus ^{6}Be, no Fermi transition is expected in the $^6_3$Li$_3$(ν_e, e^-)$^6_4$Be$_2$ reaction.

The ^{6}Li(p, n)^{6}Be CE reaction performed at $E_p = 160$ and 200 MeV [42] reports only one strong and concentrated GT transition, i.e., the ^{6}Li, 1^+ g.s. $\rightarrow$ ^{6}Be, 0^+ g.s. transition. Therefore, it is expected that only the ^{6}Be g.s. is strongly excited in the ^{6}Li(ν_e, e^-)^{6}Be CE reaction.

The Q_{EC} value is 4.29 MeV. Therefore, the ^{8}B-ν_e and hep-ν_e above this energy can be detected (see Fig. 3). The g.s. of ^{6}Be excited by the (ν_e, e^-) CE reaction decays into α and two protons.

The ^{6}Li target can detect neutrinos with all three flavors via the NC excitation of the 3.56 MeV, 0^+ state. Note that this state is the IAS of the 0^+ g.s. of ^{6}He and ^{6}Be with isospin $T = 1$. Therefore, this 0^+ state should be excited strongly from the 1^+ g.s. of ^{6}Li by the spin-$M1$ transition

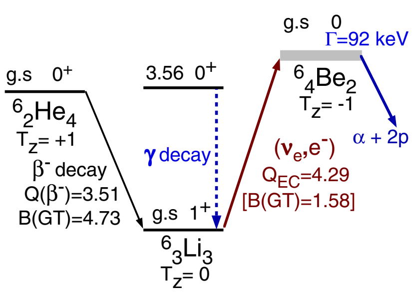

FIG. 7. Energy-level diagram and GT transitions in $A = 6$ nuclei, where $^6_2$He$_4$ and $^6_4$Be$_2$ are mirror nuclei. Properties of the excitation caused by the ^{6}Li(ν_e, e^-)^{6}Be CE reaction are indicated in red. The strength [$B(\mathrm{GT}) = 1.58$] in the square brackets, given for the GT transition from the ^{6}Li g.s. to the ^{6}Be g.s., is borrowed from that of the mirror (isospin analogous) GT transition studied in the β^- decay of the ^{6}He g.s. to the ^{6}Li g.s., where the factor of three, i.e., the difference of the relevant spin CG coefficients, is corrected.

caused by the $\sigma\tau$ operator [25]. The excitation of this state can be identified by the detection of the 3.56 MeV γ ray.

E. GT and Fermi response of $^{42}_{20}$Ca$_{22}$

Like in the $A = 18$ system, the Fermi and GT transitions starting from the e-e nucleus $^{42}_{20}$Ca$_{22}$ excite the $J^\pi = 0^+$ g.s. (the $T = 1$ IAS) and $J^\pi = 1^+$ GT states in the final nucleus $^{42}_{21}$Sc$_{21}$, respectively [37]. Again, like in the $A = 18$ system, the main part of the GT strength, i.e., $B(\mathrm{GT}) = 2.17$ is concentrated in the GT transition to the 0.61 MeV, lowest 1^+ state (see Fig. 8). Note that this state is also the LeSGT state (see the ^{42}Ca(^{3}He, t)^{42}Sc spectrum shown in Ref. [37]).

Due to the large Q_{EC} value of 6.43 MeV in the Fermi transition and that of 7.04 MeV in the GT transition, the ν_e detector using this target nucleus ^{42}Ca will be rather silent; only the higher end part of ^{8}B-ν_e and hep-ν_e can be detected (see Fig. 3).

By detecting the 0.61 MeV γ ray, the excitation of the 1^+, LeSGT state is identified. The β^+ decay of the ^{42}Sc g.s. (the IAS) can be studied by the detection of the 0.51 MeV annihilation γ.

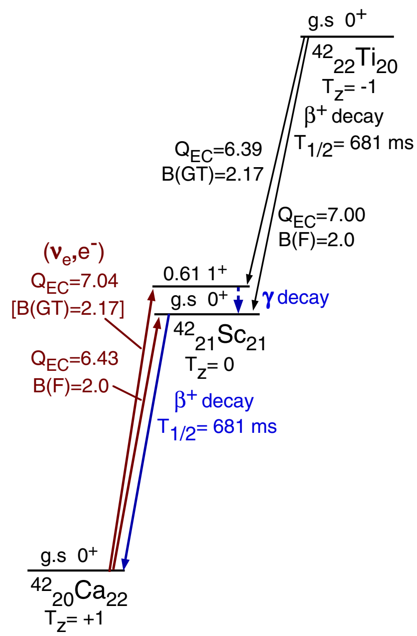

FIG. 8. Energy-level diagram and the prominent GT and Fermi transitions in $A = 42$ nuclei. Properties of excitations caused by the ^{42}Ca(ν_e, e^-)^{42}Sc CE reaction are indicated in red, while the decay properties of isospin analogous GT transitions from ^{42}Ti are shown in black. The strength [$B(\mathrm{GT}) = 2.17$] in the square brackets for the GT transition from the ^{42}Ca g.s. to the 0.61 MeV state in ^{42}Sc is borrowed from that of the mirror (isospin analogous) GT transition studied in the β^+ decay of the ^{42}Ti g.s. to the 0.61 MeV state in ^{42}Sc. Decay properties of the states in ^{42}Sc are shown in blue.

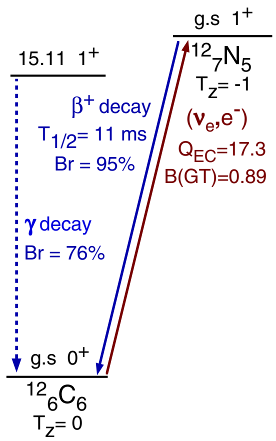

FIG. 9. Energy-level diagram and the important transitions in $A = 12$ nuclei. Properties of the GT transition caused by the $^{12}C(\nu_e, e^-)^{12}N$ CE reaction are indicated in red. The decay properties of the 1^+ g.s. of ^{12}N and its IAS at 15.11 MeV in ^{12}C are shown in blue. Note that the vertical energy scale of this diagram is reduced by a factor of two compared to those for other target nuclei.

F. GT response of $^{12}_{6}C_6$

The GT response of ^{12}C has been studied by $^{12}_{6}C_6(p,n)^{15}_{7}N_5$ experiments (see e.g., Refs. [27,28,45]). They report that the $B(\mathrm{GT})$ value of 0.89(1) concentrates in the $^{12}C, 0^+$ g.s. $\to$ $^{12}N, 1^+$ g.s. transition. No Fermi transition is expected in the CE reaction starting from the $T = T_z = 0$, e-e nucleus $^{12}_{6}C_6$. Therefore, a very simple and concentrated GT response is expected in the $^{12}C(\nu_e, e^-)^{12}N$ CE reaction (see Fig. 9).

Due to the large Q_{EC} value of 17.3 MeV, only the hep-ν_e can be selectively detected. The 1^+ g.s. of ^{12}N excited in the (ν_e, e^-) CE reaction decays back to the 0^+ g.s. of ^{12}C by the β^+ decay with an ≈95% probability. Its half-life is 11.0 ms.

The 15.11 MeV, 1^+ state of ^{12}C is the IAS of the 1^+ g.s. of ^{12}N with isospin $T = 1$. Therefore, this state should be well excited by means of the NC (in this case, by means of the $\sigma\tau$ operator) from the 0^+ g.s. of ^{12}C by the neutrinos with all flavors. The γ-decay branching ratio from this state to the g.s. is high (≈76%). The detection of this high-energy γ, however, is not easy.

V. SUMMARY AND OUTLOOK

Traditionally it has been thought that solar neutrino detectors should be capable of detecting low-energy ν_e with high intensity. For this purpose, good choices were to use target nuclei $^{A}[\mathrm{Z}]_N$ with smaller reaction Q values (Q_{EC} values) in the $^{A}[\mathrm{Z}]_N(\nu_e, e^-)^{A}[\mathrm{Z}+1]_{N-1}$ CE reaction. Taking other conditions also into account, target nuclei ^{37}Cl and ^{71}Ga were preferably selected. In particular, the Q_{EC} value of ^{71}Ga is very small; it is only 0.23 MeV. Note that this enabled the detection of low-energy pp-ν_e.

For the measurement of the $P_{ee}(E_{\nu e})$ values, i.e., the survival probability of electron neutrino ν_e as a function of its energy, however, we found that the GT and Fermi responses of these target nuclei are not ideal from a nuclear structure point of view; their GT responses are rather fragmented and also their GT strengths are all weak in the region of low excitation energy.

Progress has been made by the Borexino experiment. They use the simple $\nu_e - e^-$ elastic scattering. Therefore, in their measurement, the response for ν_es is linear as a function of $E_{\nu e}$. They reported P_{ee} values at four $E_{\nu e}$ values in the region between 0.3 to 10 MeV. Their values are consistent with the P_{ee} curve assuming the standard MSW-LMA prediction. However, their measured P_{ee} values (and also those from other experiments; see the caption of Fig. 1) are not precise enough to reject BSM physics, like the one assuming NSI.

Seeking a better determination of the P_{ee} values at different $E_{\nu e}$ values, we proposed here to use several target nuclei with different reaction Q_{EC} values, i.e., ^{7}Li, ^{18}O, ^{19}F, ^{6}Li, ^{42}Ca, and ^{12}C with the Q_{EC} values of 0.86, 1.66, 3.24, 4.29, 6.43, and 17.3 MeV, respectively. The splendid point of these target nuclei is the simple GT and Fermi responses; most of the GT and also Fermi strengths are concentrated in the low E_x region of the final nuclei, i.e., ^{7}Be, ^{18}F, ^{19}Ne, ^{6}Be, ^{42}Sc, and ^{12}N, respectively. Therefore, by using these target nuclei, we expect:

(1) ν_es with energies higher than the Q_{EC} value of each target nucleus are selectively and efficiently detected, and also
(2) the analysis to derive P_{ee} values for ν_es having above the Q_{EC} values becomes simpler, and thus more reliable.

As discussed, among these candidates of target nuclei, three of them, i.e., ^{7}Li, ^{6}Li, and ^{12}C, have large and concentrated NC responses with detection threshold energies of 0.48, 3.56, and 15.11 MeV, respectively. Note that the NC measurement, not like that of CC, is flavor independent. Therefore, the measurement should represent the original strength distribution of ν_es produced in the Sun. It is suggested that P_{ee} values can be better determined by making a combined and consistent analyses of the data from the CC and NC measurements.

In summary, we proposed several target nuclei suited for the $P_{ee}(E_{\nu e})$ measurements on the basis of nuclear structure point of view. How to realize the neutrino detectors using the proposed target nuclei is still a remaining open question. One of the recent technical options is to realize water-based liquid scintillators (WbLS) [46] loaded with these proposed isotopes. We, however, admit that further technical studies and also discussions in the scientific society are needed.

ACKNOWLEDGMENTS

Y. F. thanks the support by JSPS KAKENHI, Japan, under No. JP15K05104. K. Z. and Y. F. thanks DFG for supporting the exchange program between TU Dresden and Osaka University within the framework of the "Excellence Initiative of the German Federal and State Governments." The main part of the discussions given in this article are made on the basis of the experimental results accumulated in the high energy-resolution (^{3}He, t) measurements performed at RCNP, Osaka. The authors are indebted to the members of the accelerator group and also the Grand Raiden spectrometer group for making these experiments possible.

---

[1] W. Pauli, letter to L. Meitner, *Dear Radioactive Ladies and Gentlemen* (1930), http://cds.cern.ch/record/83282.

[2] C. F. v. Weizsäcker, Z. Phys. **38**, 176 (1937).

[3] C. F. v. Weizsäcker, Z. Phys. **39**, 633 (1938).

[4] H. A. Bethe and C. L. Critchfield, Phys. Rev. **54**, 248 (1938).

[5] H. A. Bethe, Phys. Rev. **55**, 434 (1939).

[6] B. Pontecorvo, Report PD-205, Division of Energy, Chalk River, Ontario, 1946.

[7] R. Davis, Jr., D. S. Harmer, and K. C. Hoffman, Phys. Rev. Lett. **20**, 1205 (1968).

[8] B. T. Cleveland, T. Daily, R. Davis, Jr., J. R. Distel, K. Lande, C. K. Lee, P. S. Wildenhain, and J. Ullman, Astrophys. J. **496**, 505 (1998).

[9] W. Hampel *et al.*, Phys. Lett. B **447**, 127 (1999).

[10] F. Kaether, W. Hampel, G. Heusser, J. Kiko, and T. Kirsten, Phys. Lett. B **685**, 47 (2010).

[11] M. Altmann *et al.*, Phys. Lett. B **616**, 174 (2005).

[12] J. N. Abdurashitov *et al.*, Phys. Rev. C **80**, 015807 (2009).

[13] K. Abe *et al.* (Super-Kamiokande Collaboration), Phys. Rev. D **94**, 052010 (2016).

[14] S. N. Ahmed *et al.* (SNO Collaboration), Phys. Rev. Lett. **92**, 181301 (2004).

[15] M. Agostini *et al.* (Borexino Collaboration), Nature (London) **562**, 505 (2018).

[16] M. Agostini *et al.* (Borexino Collaboration), Phys. Rev. D **100**, 082004 (2019).

[17] M. Agostini *et al.* (Borexino Collaboration), Phys. Rev. D **101**, 062001 (2020).

[18] L. Wolfenstein *et al.*, Phys. Rev. D **17**, 2369 (1978).

[19] S. P. Mikheyev and A. Yu. Smirnov, Il Nuovo Cimento C **9**, 17 (1986).

[20] S. K. Agarwalla *et al.* (Borexino Collaboration), J. High Energy Phys. 02 (2020) 038.

[21] A. Gando *et al.* (KamLAND Collaboration), Phys. Rev. C **92**, 055808 (2015).

[22] B. Aharmim *et al.* (SNO Collaboration), Phys. Rev. C **88**, 025501 (2013).

[23] A. Friedland, C. Lunardini, and C. Pena-Garay, Phys. Lett. B **594**, 347 (2004).

[24] A. Bohr and B. R. Mottelson, *Nuclear Structure*, Vol. 1 (Benjamin, New York, 1969).

[25] Y. Fujita, B. Rubio, and W. Gelletly, Prog. Part. Nucl. Phys. **66**, 549 (2011), and references therein.

[26] K. Ikeda, S. Fujii, and J. I. Fujita, Phys. Rev. Lett. **3**, 271 (1963).

[27] T. N. Taddeucci, C. A. Goulding, T. A. Carey, R. C. Byrd, C. D. Goodman, C. Gaarde, J. Larsen, D. Horen, J. Rapaport, and E. Sugarbaker, Nucl. Phys. **A469**, 125 (1987), and references therein.

[28] J. Rapaport and E. Sugarbaker, Annu. Rev. Nucl. Part. Sci. **44**, 109 (1994), and references therein.

[29] R. G. T. Zegers *et al.*, Phys. Rev. C **74**, 024309 (2006).

[30] Y. Fujita *et al.*, Phys. Rev. C **59**, 90 (1999).

[31] Y. Fujita *et al.*, Phys. Rev. C **67**, 064312 (2003).

[32] Y. Fujita *et al.*, Phys. Rev. C **75**, 057305 (2007).

[33] Y. Fujita *et al.*, Phys. Rev. Lett. **112**, 112502 (2014).

[34] F. Osterfeld, Rev. Mod. Phys. **64**, 491 (1992), and references therein.

[35] Y. Shimbara *et al.*, Phys. Rev. C **86**, 024312 (2012).

[36] H. Fujita *et al.*, Phys. Rev. C **100**, 034618 (2019).

[37] Y. Fujita *et al.*, Phys. Rev. C **91**, 064316 (2015).

[38] Y. Fujita, Y. Utsuno, and H. Fujita, Eur. Phys. J. A **56**, 138 (2020).

[39] D. Frekers *et al.*, Phys. Rev. C **91**, 034608 (2015).

[40] Nuclear Data Evaluation Project, Triangular Universities Nuclear Laboratory: https://nucldata.tunl.duke.edu/.

[41] Evaluated Nuclear Structure Data File, National Nuclear Data Center, Brookhaven National Laboratory: https://www.nndc.bnl.gov/ensdf/.

[42] J. Rapaport *et al.*, Phys. Rev. C **41**, 1920 (1990).

[43] J. Rapaport, C. Gaarde, J. Larsen, C. Goulding, C. D. Goodman, C. Foster, D. J. Horen, T. Masterson, E. Sugarbaker, and T. N. Taddeucci, Nucl. Phys. **A431**, 301 (1984).

[44] D. Kahl *et al.*, Eur. Phys. J. A **55**, 4 (2019).

[45] B. D. Anderson, L. A. C. Garcia, D. J. Millener, D. M. Manley, A. R. Baldwin, A. Fazely, R. Madey, N. Tamimi, J. W. Watson, and C. C. Foster, Phys. Rev. C **54**, 237 (1996).

[46] M. Yeh, S. Hans, W. Beriguete, R. Rosero, L. Hu, R. L. Hahn, M. V. Diwan, D. E. Jaffe, S. H. Kettell, and L. Littenberg, Nucl. Instrum. Methods Phys. Res., Sect. A **660**, 51 (2011).